scientific reports

Check for updates

OPEN

Dynamic alterations in cortical activation during motor adaptation in table tennis using whole-brain fNIRS

Daniel Carius [1] ✉, Elisabeth Kaminski [1,2], Martina Clauß [1] & Patrick Ragert [1,2]

Human movements must constantly be adapted due to changing internal and external conditions in our environment. The underlying neuronal mechanisms that are responsible for motor adaptations have so far mainly been investigated in highly controlled laboratory scenarios using simple motor tasks. However, because motor adaptations in daily life and sports entail more complex processes involving several cognitive components and strategic adjustments, results from such highly controlled settings only allow restricted conclusions and do not capture neuronal processing in everyday life scenarios. Hence, we studied 56 participants using a table tennis paradigm to unravel cortical activation during motor adaptation in a sport-specific setting using functional NIRS. Furthermore, we wanted to investigate whether cortical activation during motor adaptation is influenced by the temporal order of perturbations (serial vs. randomized practice). Our findings revealed brain areas such as the dorsolateral prefrontal cortex and primary sensory cortex, left supplementary motor cortex and left primary motor cortex, as well as right superior parietal cortex and right inferior parietal cortex, exhibited dynamic alterations in their activation as motor adaptation progressed. Specifically, hemodynamic response alterations generally increased during early adaptation and decreased as motor adaptation progressed. On the other hand, no differential changes in cortical brain processing were observed with serial and randomized practice. Based on our findings, we can confirm and extent theoretical models and laboratory evidence of motor adaptation using a sport-specific motor task.

Keywords Motor adaptation, Neuroplasticity, Near-infrared spectroscopy, Whole-brain, Table tennis

Human movements frequently require ongoing motor adaptations due to a changing environment. These adaptations represent new sensorimotor relationships and form the basis for human motor behavior. In contrast to new movement skills, adapting already learned internal models to changing physical conditions or new environmental circumstances represent fast learning processes. These adaptational processes usually require only minor changes to previously learned movements[1–5]. Underlying neural mechanisms that are responsible for such adaptations have so far mainly been investigated in highly controlled laboratory settings using EEG or fMRI. However, these methodological approaches allow only limited conclusions for everyday scenarios as motor adaptations in everyday life involve more complex, often non stationary movement patterns with various cognitive components and strategic corrections[6,7]. In the present study, we used a naturalistic motor adaptation paradigm[8] to unravel hemodynamic response alteration, defined as cortical activation, during motor adaptation in a sport-specific table tennis setting.

Background on motor adaptation

In general, two mechanisms are involved in motor adaptation: explicit learning driven by target error and implicit learning of a forward model driven by prediction error[9]. During the initial phase of adaptation, predominantly explicit learning takes place in order to minimize target errors. This fast process is followed by slow implicit learning, which gradually updates the sensorimotor mapping. When perturbations disappear after a new sensorimotor mapping, transient after-effects occur, which again represent target errors in the direction opposite to the initial sensorimotor conflict. These after-effects are considered evidence for an adapted internal model that initially persists when perturbation ends[10]. There are two classic approaches that make motor

[1]Department of Movement Neuroscience, Faculty of Sport Science, Leipzig University, 04109 Leipzig, Germany. [2]Max Planck Institute for Human Cognitive and Brain Sciences, 04103 Leipzig, Germany. ✉email: daniel.carius@uni-leipzig.de

adaptations experimentally accessible. In force-field adaptation tasks[1,2,5,11–14], the execution of the movement is disturbed by an additional or altered external force. In contrast, visuomotor rotation tasks[3,4,9,15–18] do not disturb the execution of the movement itself, but the subsequent movement-effect relationship. This creates a mismatch between vision and proprioception that requires adaptations such that individuals have to modify their motor output to account for the respective perturbation and resolve the sensorimotor conflict. In real life scenarios, motor adaptations are sparsely investigated. We recently investigated motor adaptation using a table tennis paradigm. Here, a table tennis robot changed its ball spin during the course of adaptation phases. These environmental changes require sensorimotor adaptations to update the movement-effect relationship while movement execution is not directly affected. In summary, we were able to show that our paradigm reflects typical motor adaptations in a sport-specific context[8]. Furthermore, we observed that on a behavioral level, temporal ordering of the perturbations (serial vs. random practice) had no influence on motor adaptation performance. However, temporal ordering could still induce differential brain processing due to differences in cognitive effort or motivation. Lage et al.[19] suggested that, despite comparable behavioral performances between serial and random practice schedules, mental resources required for each task may differ. This perspective aligns with findings[20] indicating that constant and random practice schedules elicit distinct EEG patterns. However, whether serial and random perturbations within our paradigm also produce differential neural activity remains an open question.

Brain processing during motor adaptation

Evidence from both theoretical models and empirical studies concluded that cerebellar, striatal and neocortical structures such as primary motor cortex (M1), premotor cortex (PMC), dorsolateral prefrontal cortex (DLPFC) and supplementary cortex (SMA) as well as parietal cortex show dynamic alterations during visuomotor adaptation[5,17,21–23]. The cortico-striatal circuit particularly contributes during early motor adaptation, whereas the cortico-cerebellar circuit plays a more critical role during later phases[22]. Among these brain structures, the posterior parietal cortex (PPC) seems to be of particular relevance for successful motor adaptation[7,24]. In general, brain processing increases as a response to a sudden exposure to a perturbation (e.g., visuomotor rotation). On the other hand, brain processing decreases as visuomotor adaptation progresses, and increases again when the perturbation is suddenly removed[17]. These neuronal mechanisms of motor adaptations have mainly been observed using functional magnetic resonance imaging[25,26]. However, Yeo et al.[7] pointed out that motor adaptation studies using fMRI are usually performed in a supine position due to structural limitations. Since posture directly affects sensorimotor integration and adaptation due to altered somatosensory and vestibular input and only a limited amount of movement is possible during fMRI measurements, one might argue that neural correlations of motor adaptation using fMRI do not necessarily generalize to correlates of adaptations in everyday movements[6,7]. In a recent study, fNIRS was used to investigate changes in cortical activation during motor adaptation in a spatial orientation task[7]. The study showed, that fNIRS in general seems to be feasible to unravel changes in brain processing as a consequence of motor adaptation[7]. However, many everyday and sport-specific motor adaptations take place in non-stationary motor conditions, e.g., during walking. These result from Yeo et al. can therefore not necessarily be generalized to everyday life scenarios or a sport-specific context.

A large number of studies have shown that fNIRS is in fact suitable for investigating cortical activation during the execution of controlled everyday life and sport-specific movements while standing and walking[27,28]. In the present study, we used a table tennis paradigm[8] to unravel cortical activation during motor adaptation in a sport-specific table tennis setting and to differentiate between temporal order of perturbations. We hypothesized that (a) cortical structures, that are important for motor adaptation such as bilateral M1, PMC, SMA, DLPFC and PPC[5,7,17,21–23] dynamically alter their activation as motor adaptation progresses. In addition, we hypothesized that (b) hemodynamic response alterations increase during early adaptation, decrease as visuomotor adaptation progresses, and increases again when the rotation is suddenly removed[17]. Furthermore, we hypothesized that (c) serial and randomized practice lead to comparable motor adaptation performances[8,19] with higher cortical activation during serial compared to random practice[19]. According to the elaboration hypothesis, serial practice demands greater working memory load and sequence integration compared to an unforeseen practice schedule during random practice[19]. Thus, increased cortical activation is expected mainly in the prefrontal cortex, posterior parietal cortex and supplementary motor area, since these regions are mainly involved in cognitive control, motor planning, and sequence coordination[22,24,29].

Material and methods
Participants

We recruited a total of 66 participants. Five participants had to be excluded due to missing data, two participants due to pain and three participants due to issues with the robot. Thus, 56 right-handed healthy volunteers, with an average age of 22.30 ± 2.26 years, ranging from 19 to 27 years old (25 female participants) were included in the present study. The study procedure was approved by the local ethics committee of the University of Leipzig (309/17-ek). Every participant gave written, informed consent, and every procedure followed the guidelines set forth in the Declaration of Helsinki. None of the participants had a history of neurological, psychiatric, cardiovascular, or musculoskeletal diseases, nor had they taken centrally acting medications. To evaluate the effects of motor adaptation during serial and random perturbation situations, participants were randomly divided in two groups. In order to rule out any significant differences between groups with regard to potential confounders, the number of hours that each group spent on sports and fine motor training each week were quantified (see Table 1). All volunteers were found to be right-handed based on the Edinburgh Handedness Questionnaire[30] with a mean handedness score of 81.65 ± 1.90. The cut-off score of ≥ 50 indicated right-handedness, ≤ − 50 showed left-handedness, and ≥ − 50 indicated ambidextrous handedness[31]. Furthermore, we ensured that each participant was a novice table tennis player who had not taken part in regular table tennis

Group	Age (years)	Gender (female/male)	LQ (score)	Sports/week (hours)	Fine-motor training/week (hours)
Serial n = 29	22.38 ± 0.43	14/15	82.21 ± 2.45	4.85 ± 0.47	3.22 ± 0.68
Random n = 27	22.22 ± 0.43	10/17	81.04 ± 2.99	4.96 ± 0.56	2.63 ± 0.47

Table 1. Group demographics. *LQ* laterality quotient as assessed with the Edinburgh Handedness Scale [range: −100 (full left-handed) to +100 (full right-handed)]. Hours of sports per week and hours of fine motor training per week (e.g., playing a musical instrument, knitting, doing handcrafts, playing video games with a keypad or joystick) were assessed with a questionnaire. All values are depicted as standard error (SE) of the mean. Statistical analysis revealed no differences in age ($U = 403.5$, $p = 0.849$), gender ($\chi^2 = 0.72$, $p = 0.396$), LQ ($U = 407.5$, $p = 0.798$), sports/week ($U = 401.0$, $p = 0.882$), or fine-motor training/week ($U = 401.0$, $p = 0.881$) between groups.

training before. However, participants still needed to be able to execute the required movement skill—the backhand stroke—sufficiently well in predefined, simple conditions (without perturbations). To make sure that participants satisfied this need, we employed a pretest with a predetermined target accuracy (see the following section). The amount of time spent on sports (a) and fine motor training (b) per week—such as playing video games, knitting, crocheting, or playing an instrument—was measured using a standardized questionnaire. All participants completed a visual analog scale (VAS) before and after the experiment to rate their level of attention (1 (very distracted)—10 (very attentive)), fatigue (1 (sleeping)—10 (very energetic)), and discomfort (1 (no discomfort)—10 (strong discomfort))) in order to account for potential psychological confounders.

Experimental procedure

In the present study, we used a table tennis paradigm[8] to unravel cortical activation during motor adaptation in a sport-specific setting (Fig. 1a). Participants performed backhand strokes (BH) cross-court against balls played by an app-controlled table tennis robot (Donic Newgy Robo-Pong 3050XL, Germany). During baseline and washout blocks participants performed BH against topspin balls. During adaptation blocks, participants performed BH against backspin balls, representing disturbances in terms of motor adaptation (see Fig. 1b,c). In contrast to our previous study[8], we standardized the number of task switches for both conditions to improve the comparability of the two protocols. In the current study, we induced eight task switches in both random order and serial order condition (As-As-Al-Al-As-As, As: short ball, Al: long ball) with 16 balls per block being played. BH strokes were executed according to a block design for 20 × 32 s (jittered intertrial interval 35–40 s, 16 balls per block, see Fig. 1c,d), whereby participants were instructed to perform strokes as accurately as possible.
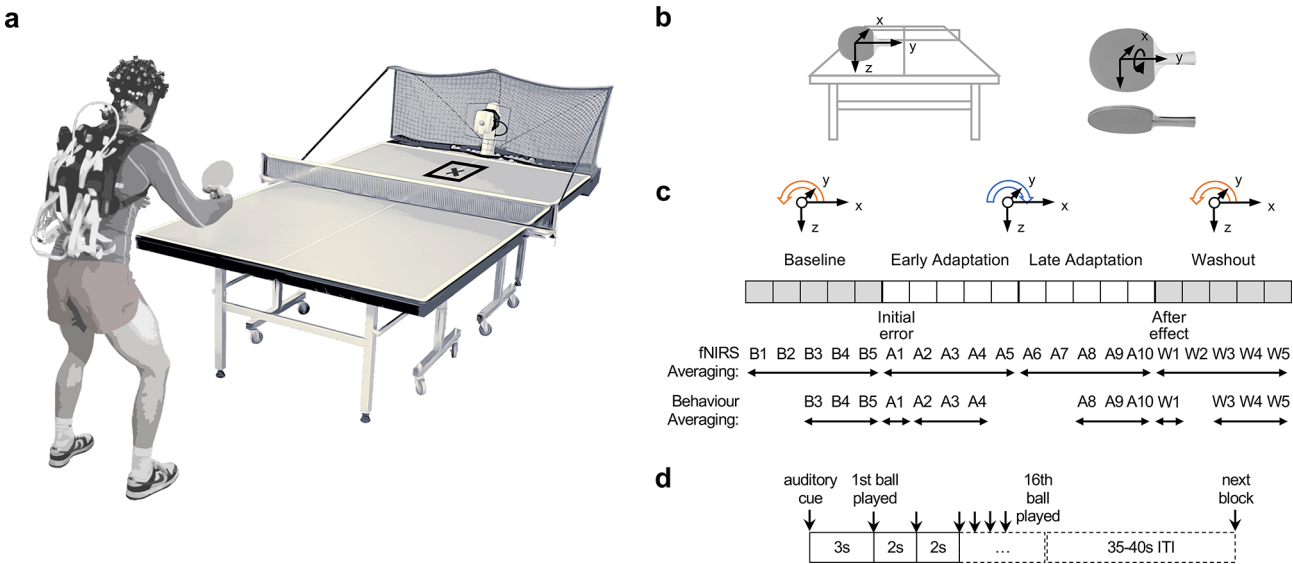

Fig. 1. Experimental setup and protocol. (**a**) Positioning of app-controlled ball robot at table tennis plate. Target marked with a cross. Participant in backhand stroke (BH) position carrying the fNIRS system. Photo editing was done using Adobe Photoshop (2024, v. 25) (**b**) Reference system of the racket. Translational movement in x-direction (left panel). Motor adaptation around transversal y-axis (right panel). (**c**) Experimental flow. Ball rotation changes (around transversal y-axis) in the course of adaptation phases. During baseline blocks participants performed BH against topspin balls (orange arrow). During adaptation blocks, participants performed BH against backspin balls (blue arrow), representing disturbances in terms of motor adaptation. In the last five blocks (washout) BH was performed against top spin balls, again. Averaging windows for the behavioral and fNIRS analysis are shown below the block diagram. (**d**) Each block consists of 16 trials (32 s). Blocks were separated by 35–40 s jittered intertrial intervals (ITI).

Onsets of blocks were indicated via an auditory stimulus (short tone) and fNIRS triggers were set via Psychopy[32]. Motor adaptation was evaluated by means of target accuracy. 2D cinematography was used to determine the placement of participants' balls. Target accuracy alterations due to adaptation were assessed and distances to the target were computed. Analog to our previously established procedure[8], target accuracy was recorded with a high-speed video camera (GoPro Hero 9, San Mateo, US, 1920 × 1080 pixel, 200 frames per second,) and ball placement on the table tennis table was measured offline using Kinovea (v0.9.5, GPL-2.0 license).

Functional near-infrared spectroscopy (fNIRS)

Hemodynamic responses were recorded using a whole-brain fNIRS system (NIRSport2, NIRX, US). Measurement requirements and fNIRS setup with 32 LED light sources and 32 avalanche photodiode detectors were used analog to Carius et al.[33]. In contrast to our previous study, we used additional washers for avalanche photodiodes (APD). These APD washers (diameter 2.5 cm) are intended to stabilize the APDs and prevent optodes from tilting. To ensure that washers fit under all optodes, we slightly modified the placement of the fNIRS optodes resulting in a more symmetrical configuration (106 actual measurement channels, see Fig. 2). In addition to the 106 (standard) channels, we also used eight short-distance detectors (NIRx Medical Technologies, Glen Head, NY) to exclude potential fNIRS confounders, such as changes in extracerebral blood flow. Data were acquired with a sampling frequency of 10.1725 Hz. To rule out expertise-related differences, we measured cardiac stress, operationalized via heart rate, during the execution of table tennis strokes using a Polar M430 sport watch (Polar Electro Oy, Kempele, Finland) with a sampling frequency of 1 Hz.

Data analyses

Behavioral data

Pythagorean theorem was used to calculate distances between hit points and target point. Distances and centroids, representing direction of deviations, were calculated for each participant and each block[8]. Data analysis and statistical analyses were performed using MATLAB (Version R2023a, MathWorks, Natick, MA, United States of America), RStudio (Version 2023.9.0.463, RStudio Team 2023) and JASP (Version 0.17, JASP Team 2021). Mean
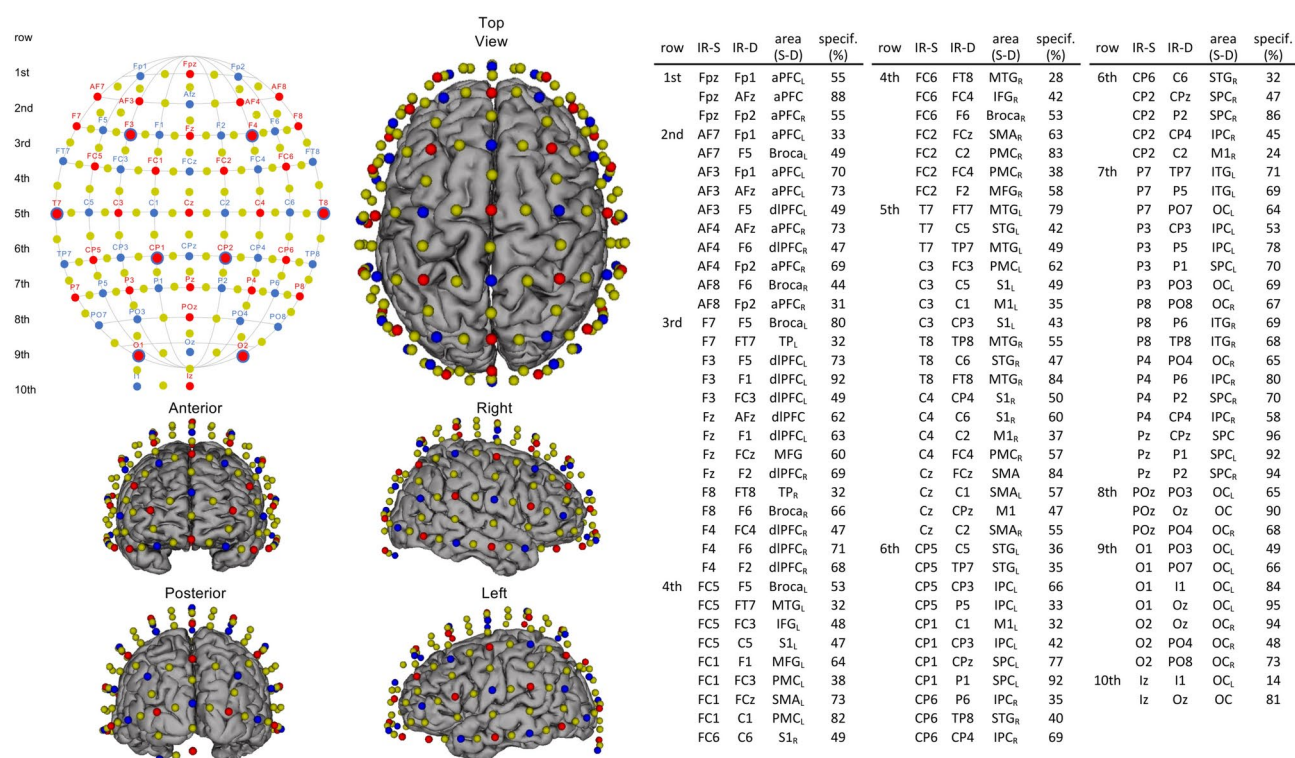

row	IR-S	IR-D	area (S-D)	specif. (%)	row	IR-S	IR-D	area (S-D)	specif. (%)	row	IR-S	IR-D	area (S-D)	specif. (%)
1st	Fpz	Fp1	$aPFC_L$	55	4th	FC6	FT8	MTG_R	28	6th	CP6	C6	STG_R	32
	Fpz	AFz	$aPFC$	88		FC6	FC4	IFG_R	42		CP2	CPz	SPC_R	47
	Fpz	Fp2	$aPFC_R$	55		FC6	F6	$Broca_R$	53		CP2	P2	SPC_R	86
2nd	AF7	Fp1	$aPFC_L$	33		FC2	FCz	SMA_R	63		CP2	CP4	IPC_R	45
	AF7	F5	$Broca_L$	49		FC2	C2	PMC_R	83		CP2	C2	$M1_R$	24
	AF3	Fp1	$aPFC_L$	70		FC2	FC4	PMC_R	38	7th	P7	TP7	ITG_L	71
	AF3	AFz	$aPFC_L$	73		FC2	F2	MFG_R	58		P7	P5	ITG_L	69
	AF3	F5	$dlPFC_L$	49	5th	T7	FT7	MTG_L	79		P7	PO7	OC_L	64
	AF4	AFz	$aPFC_R$	73		T7	C5	STG_L	42		P3	CP3	IPC_L	53
	AF4	F6	$dlPFC_R$	47		T7	TP7	MTG_L	49		P3	P5	IPC_L	78
	AF4	Fp2	$aPFC_R$	69		C3	FC3	PMC_L	62		P3	P1	SPC_L	70
	AF8	F6	$Broca_R$	44		C3	C5	$S1_L$	49		P3	PO3	OC_L	69
	AF8	Fp2	$aPFC_R$	31		C3	C1	$M1_L$	35		P8	PO8	OC_R	67
3rd	F7	F5	$Broca_L$	80		C3	CP3	$S1_L$	43		P8	P6	ITG_R	69
	F7	FT7	TP_L	32		T8	TP8	MTG_R	55		P8	PO8	OC_R	68
	F3	F5	$dlPFC_L$	73		T8	C6	STG_R	47		P4	PO4	OC_R	65
	F3	F1	$dlPFC_L$	92		T8	FT8	MTG_R	84		P4	P6	IPC_R	80
	F3	FC3	$dlPFC_L$	49		C4	CP4	$S1_R$	50		P4	P2	SPC_R	70
	Fz	AFz	$dlPFC$	62		C4	C6	$S1_R$	60		P4	CP4	IPC_R	58
	Fz	F1	$dlPFC_L$	63		C4	C2	$M1_R$	37		Pz	CPz	SPC	96
	Fz	FCz	MFG	60		C4	FC4	PMC_R	57		Pz	P1	SPC_L	92
	Fz	F2	$dlPFC_R$	69		Cz	FCz	SMA	84		Pz	P2	SPC_R	94
	F8	FT8	TP_R	32		Cz	C1	SMA_L	57	8th	POz	PO3	OC_L	65
	F8	F6	$Broca_R$	66		Cz	CPz	$M1$	47		POz	Oz	OC	90
	F4	FC4	$dlPFC_R$	47		Cz	C2	SMA_R	55		POz	PO4	OC_R	68
	F4	F6	$dlPFC_R$	71	6th	CP5	C5	STG_L	36	9th	O1	PO3	OC_L	49
	F4	F2	$dlPFC_R$	68		CP5	TP7	STG_L	35		O1	PO7	OC_L	66
4th	FC5	F5	$Broca_L$	53		CP5	CP3	IPC_L	66		O1	I1	OC_L	84
	FC5	FT7	MTG_L	32		CP5	P5	IPC_L	33		O1	Oz	OC_L	95
	FC5	FC3	IFG_L	48		CP1	C1	$M1_L$	32		O2	Oz	OC_R	94
	FC5	C5	$S1_L$	47		CP1	CP3	IPC_L	42		O2	PO4	OC_R	48
	FC1	F1	MFG_L	64		CP1	CPz	SPC_L	77		O2	PO8	OC_R	73
	FC1	FC3	PMC_L	38		CP1	P1	SPC_L	92	10th	Iz	I1	OC_L	14
	FC1	FCz	SMA_L	73		CP6	P6	IPC_R	35		Iz	Oz	OC	81
	FC1	C1	PMC_L	82		CP6	TP8	STG_R	40					
	FC6	C6	$S1_R$	49		CP6	CP4	IPC_R	69					

Fig. 2. fNIRS configuration used during motor adaptation. Transmitters are shown as red dots and detectors as blue dots. Yellow dots represent each center of the 106 channels (inter-optode distance 35.8 ± 3.9 mm). Short-distance detectors are shown as blue circles surrounding the corresponding transmitters (8 mm distance from F3, F4, T7, T8, CP1, CP2, O1, O2). 10–20 positions for infrared sources (IR-S) and detectors (IR-D). Brain image was created with brain function mapping tool[34]. Respective brain regions, targeted by a 10–20 system transfer method[35] and defined by the "Brodmann" Atlas (*aPFC* anterior prefrontal cortex, *Broca* broca area, *dlPFC* dorsolateral prefrontal cortex, *IFG* inferior frontal gyrus, *IPC* inferior parietal cortex, *ITG* inferior temporal gyrus, *M1* primary motor cortex, *MFG* middle frontal gyrus, *MTG* middle temporal gyrus, *OC* occipital cortex, *PMC* premotor cortex, *S1* primary somatosensory cortex, *SMA* supplementary motor cortex, *SPC* superior parietal cortex, *STG* superior temporal gyrus, *TP* temporal pole; *L* left hemisphere, *R* right hemisphere).

distances of blocks B3 to B5 (baseline), A2 to A4 (early adaptation), A8 to A10 (late adaptation), and W3 to W5 (washout) were averaged for statistical examination of adaptation-related performance changes. Mean distances of A1 indicate initial error at the beginning of the perturbation, while mean distances of W1 indicate after-effect. Direction of changes in target accuracy during baseline, perturbation, adaptation, after-effects, and washout are represented by density plots[8]. A 6 (time)×2 (group) mixed ANOVA with post-hoc testing (i.e., T-tests) was used to examine target accuracy during 1) baseline, 2) initial error, 3) early adaptation, 4) late adaptation, 5) after-effect and 6) washout (see Fig. 1c) for the perturbation groups (serial vs. random). Data were spherically corrected, if needed, using the Greenhouse–Geisser adjustment. The problem of multiple comparisons was mitigated by the application of Holm adjustment.

Hemodynamics
FNIRS data analysis was performed in MATLAB using HOMER3 (version 1.80.2)[36] and QT-NIRS[37]. We used QT-NIRS[37] to estimate the fNIRS data quality. According to our previously established procedure[33] ($F_{minmax} = [0.5\ 2.5]$; wLength = 3; sciThld = 0.7; pspThld = 0.1), 18 participants had to be excluded. The remaining participants ($n = 38$) showed good data quality for 81.8% of the channels. As a next step, the raw intensity signals were converted to changes in optical density[36]. Wavelet filtering was used to correct for motion artifacts[38,39]. We employed the HOMER3 hmrR_MotionCorrectWavelet filtering function (inter-quartile range 1.22[40]) and the approach outlined by Molavi and Dumont[41]. The data was slightly low-pass filtered with a low pass cutoff frequency of 3 Hz after motion-artifact correction. Since the following GLM tackles this with a polynomial drift correction, we did not employ a high pass filter. Using the modified Beer-Lambert technique (partial pathlength factor: 6.0[36]), attenuation variations of both wavelengths (850 nm and 760 nm) were converted to concentration changes of oxy- and deoxygenated hemoglobin (HbO and HbR, respectively). As advised in the current literature[42], we report both HbO and HbR (rather than just one chromophore changes). However, HbO and HbR reflect distinct neurophysiological processes related to brain activity. While HbO primarily reflects changes in blood supply, HbR is directly linked to the process of oxygen extraction from the blood[43]. HbO often exhibits larger signal changes and is therefore frequently the main focus of fNIRS studies. However, since HbR concentration changes (i) are less affected by systemic physiological noise[44,45], (ii) have a stronger correlation with the blood oxygen level-dependent signal of the functional magnetic resonance imaging[46,47], and (iii) are spatially more focused[44,48], we primarily, though not solely, focus on the HbR parameter in the results and discussion section.

We used a general linear model approach (GLM) that employs ordinary least squares and a series of Gaussian functions with a standard deviation of 0.5 s and their means separated by 0.5 s over a specific regression time to model the hemodynamic response function (HRF) in order to regress extra-cerebral contaminations (measured by short-distance channels) out of the signal (used parameters in HOMER3 hrmR_GLM function: trange −2.0 to 40; glmSolveMethod 1; idxBasis 1; paramBasis 0.5 and 0.5). Additionally, we employed a third order polynomial fit to take baseline drift into consideration. The short separation channel, which exhibits the strongest correlation with the corresponding long-separation channel[49,50], is used for short separation regression (SSR). Time courses of changes in HbO and HbR concentrations in each measurement channel and condition were block-averaged, and single trials were baseline corrected with respect to the two seconds before to stimulus initiation. For TFCE analysis, the complete HbO and HbR time courses were exported.

Statistical Analyses were performed using nonparametric threshold-free cluster enhancement (TFCE, Carius, et al.[33]) with a cluster threshold of $p = 0.05$[51,52] and 10.0000 permutations. TFCE tests were conducted in MATLAB using the TFCE-Toolbox[51]. Differences in HbO and HbR concentration changes between motor adaptation phases (baseline vs. early adaptation vs. late adaptation vs. washout) and perturbation groups (serial vs. random) were tested using TFCE mixed two-way ANOVA (default TFCE parameters: E = 2/3, H = 1, Mensen and Khatami[51], Smith and Nichols[52]). In the case of non-significant interactions, we conducted post hoc tests for the main effects time and group. For the factor time, we used dependent sample TFCE T-Tests (default parameters: E = 2/3, H = 2). For factor group we used independent sample TFCE T-Tests (default parameters: E = 2/3, H = 2).

We report cluster sizes (the number of significant channels and/or time points), corrected p-values and TFCE t-values for the peak coordinates of the resulting clusters. We temporally averaged TFCE t-values[33] for all channels in the sample range 5 to 32 s in order to illustrate the task-related changes. Finally, we mapped them onto the brain surface using the brain function mapping tool[34]. Spatio-temporal clusters are printed as color-coded T-maps in time and space (106 channels).

Results
Behavioral data
In terms of target accuracy, there was no interaction between time (baseline vs. initial error at perturbation onset vs. early vs. late adaptation vs. after-effects vs. washout) and perturbation (serial vs. random, $F(2.54, 136.92) = 2.76$, $p = 0.054$, $\eta_p^2 = 0.05$). We also identified no differences between types of perturbation ($F(1, 54) = 1.06$, $p = 0.307$, $\eta_p^2 = 0.02$). Thus, temporal order of perturbations did not influence motor adaptation. In contrast, we identified adaptation-dependent differences in target accuracy comparing baseline, initial error at perturbation onset, early and late adaptation, after-effects and washout across groups ($F(2.54, 136.92) = 147.06$, $p < 0.001$, $\eta_p^2 = 0.73$). Post hoc tests revealed an increase in target errors at perturbation onset (baseline (B3-B5)—initial error (A1), $M_{diff} = -114.14$, $t(55) = -22.42$, $p_{holm} < 0.001$, $d = -3.85$), significant early adaptation (initial error (A1)—early adaptation (A2-A4), $M_{diff} = 68.18$, $t(55) = 13.39$, $p_{holm} < 0.001$, $d = 2.30$) and late adaptation effects (early adaptation (A2–A4)—late adaptation (A8–A10), $M_{diff} = 27.13$, $t(55) = 5.33$, $p_{holm} < 0.001$, $d = 0.91$). We observed large target errors when perturbations ends (late adaptation (A8-A10)—after-effect (W1), $M_{diff} = -46.53$, $t(55) = -9.14$, $p_{holm} < 0.001$, $d = -1.57$) and subsequently significant washout (after-effects (W1)—
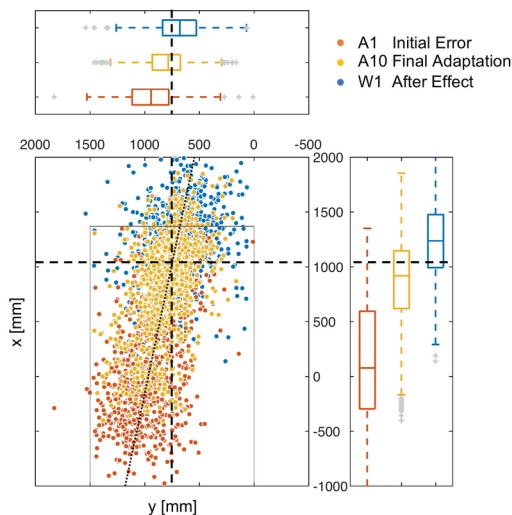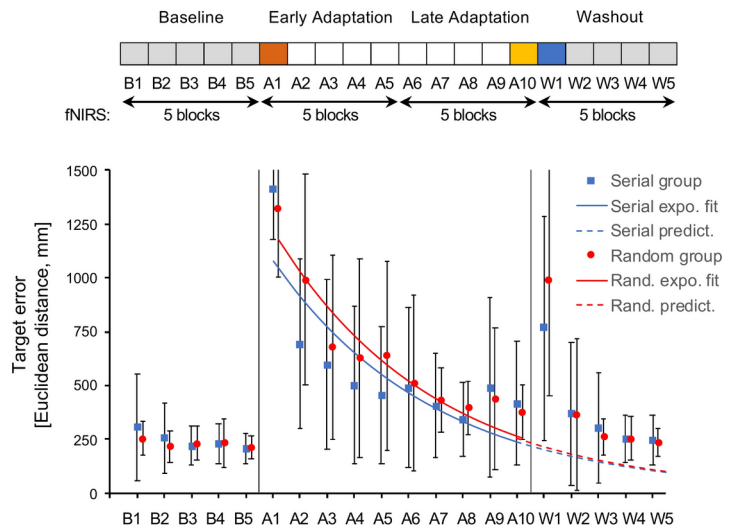
a Initial Error, Final Adaptation & After Effect   **b** Target error across motor adaptation phases

Fig. 3. Motor adaptation assessed with table tennis paradigm. (**a**) Dot plot illustrates target error dispersions during initial error (block A1) at perturbation onset, final adaptation (block A10) and after effect (block W1). Display of hit points across 56 participants (896 trials per block: 56 participants × 16 trials). Dottet line represents linear trend. Intersection of dashed lines represents target. Box plots illustrate block-related dispersions in vertical and horizontal direction. Dashed lines show target in vertical and horizontal direction. During perturbation onset majority of balls were played too short resulting in large initial errors (orange). In contrast, when perturbation disappears, majority of balls were played too long resulting in target errors in opposite direction (after effect, blue). Gray box illustrates table tennis table. Hit points outside the table were calculated using data-driven linear model[33]. (**b**) Dot plots and line plots (exponential curve fit: $y = a \cdot e^{b \cdot x}$; y = Target error, x = Block; Random group: $139 \cdot e^{-0.17\,Block}$; $R^2 = 0.91$; Serial group: $127 \cdot e^{-0.17\,Block}$; $R^2 = 0.66$) showing adaptation-dependent performance changes in terms of spatial deviation from target (Euclidean distance) for random and serial group (lower panel). Double arrows below the block diagram illustrate the included data of the phase-related fNIRS block averages (upper panel).

washout (W3-W5), $M_{diff} = 61.69$, $t(55) = 12.12$, $p_{holm} < 0.001$, $d = 2.08$). During perturbation onset, the majority of balls were played too short resulting in large target errors. In contrast, when perturbation disappears, majority of balls were played too long resulting in target errors in opposite direction (see Fig. 3a,b).

Hemodynamics

Nonparametric cluster-based permutation analysis (TFCE) revealed no interactions between motor adaptation phases (baseline vs. early adaptation vs. late adaptation vs. washout) and type of perturbation (serial vs. random), neither for HbO (peak significance found at OC_R: $F(1,144)_{max} = 5.47$, $p_{max} = 0.486$, FWE TFCE-corrected), nor for HbR (ITG_R: $F(1,144)_{max} = 5.07$, $p_{max} = 0.726$). Additionally, we did not find significant effects for perturbation (HbO, $dlPFC_R$: $F(1,144)_{max} = 10.18$, $p_{max} = 0.532$, HbR, MTG_R: $F(1,144)_{max} = 8.93$, $p_{max} = 0.799$). In contrast, cluster-based permutation tests indicated differences between motor adaptation phases (HbO peak significance found at $Broca_L$: $F(3,144)_{max} = 17.71$, $p_{max} < 0.001$, HbR peak significance found at $Broca_L$: $F(3,144)_{max} = 14.43$, $p_{max} < 0.001$).

TFCE post hoc comparisons of HbR concentration changes indicated higher cortical activation during early adaptation compared to baseline in a widespread cluster ($S1_L$, $t(37)_{max} = 6.09$, $p_{max} < 0.001$) including $S1_L$, $dlPFC_L$, SMA_L, STG_R, $S1_R$, SPC_R, $dlPFC_R$, $Broca_R$, PMC_R, MTG_R, STG_L, OC_R, MTG_L, PMC_L, $M1_L$, $Broca_L$, IPC_R, $M1_R$ & SMA_R (76 channels, sorted by temporally aggregated TFCE t-values in descending order, Fig. 4a shows temporal aggregated difference maps for TFCE t-values, Range 5–32 s, and HbO & HbR grand-averages for ROIs with highest t-values). In contrast, the comparison of early and late adaptation indicated lower cortical activation during late adaptation compared to early adaptation in a widespread cluster ($dlPFC_R$, $t(37)_{max} = -5.20$, $p_{max} < 0.001$) including $dlPFC_L$, $dlPFC_R$, $M1_R$, SMA_L, SMA_R, $M1_L$, PMC_L, SPC_R, PMC_R, $aPFC_L$, $S1_R$, IPC_R, $S1_L$, MTG_R, $aPFC_R$, IPC_L & SPC_L (50 channels, sorted by TFCE t-values in descending order, Fig. 4b shows grand-averages for ROIs as well as temporal aggregated difference maps for all TFCE t-values, Range 5–32 s). Finally, TFCE analysis indicated lower cortical activation during deadaptation/washout compared to late adaptation ($dlPFC_R$, $t(37)_{max} = -4.46$, $p_{max} < 0.001$, cluster including IPC_R, IPC_L, OC_R, SPC_L, $S1_L$, $aPFC_R$, $dlPFC_L$, $aPFC_L$, SPC_R, $M1_L$, SMA_R, $S1_R$, STG_R, MTG_R, SMA_L, $dlPFC_R$, STG_L, MTG_L, OC_L, PMC_R & PMC_L (73 channels, sorted by TFCE t-values in descending order). Summarizing TFCE post hoc comparisons of HbR concentration changes (TFCE t-values summed across time phases: baseline vs. early adaptation, early vs. late adaptation, late adaptation vs. washout), largest overall adaptation-related changes were observed for $dlPFC_L$, SMA_L, $dlPFC_R$, $S1_L$, SPC_R, $M1_L$, $S1_R$, IPC_R, & OC_R (Fig. 4c).
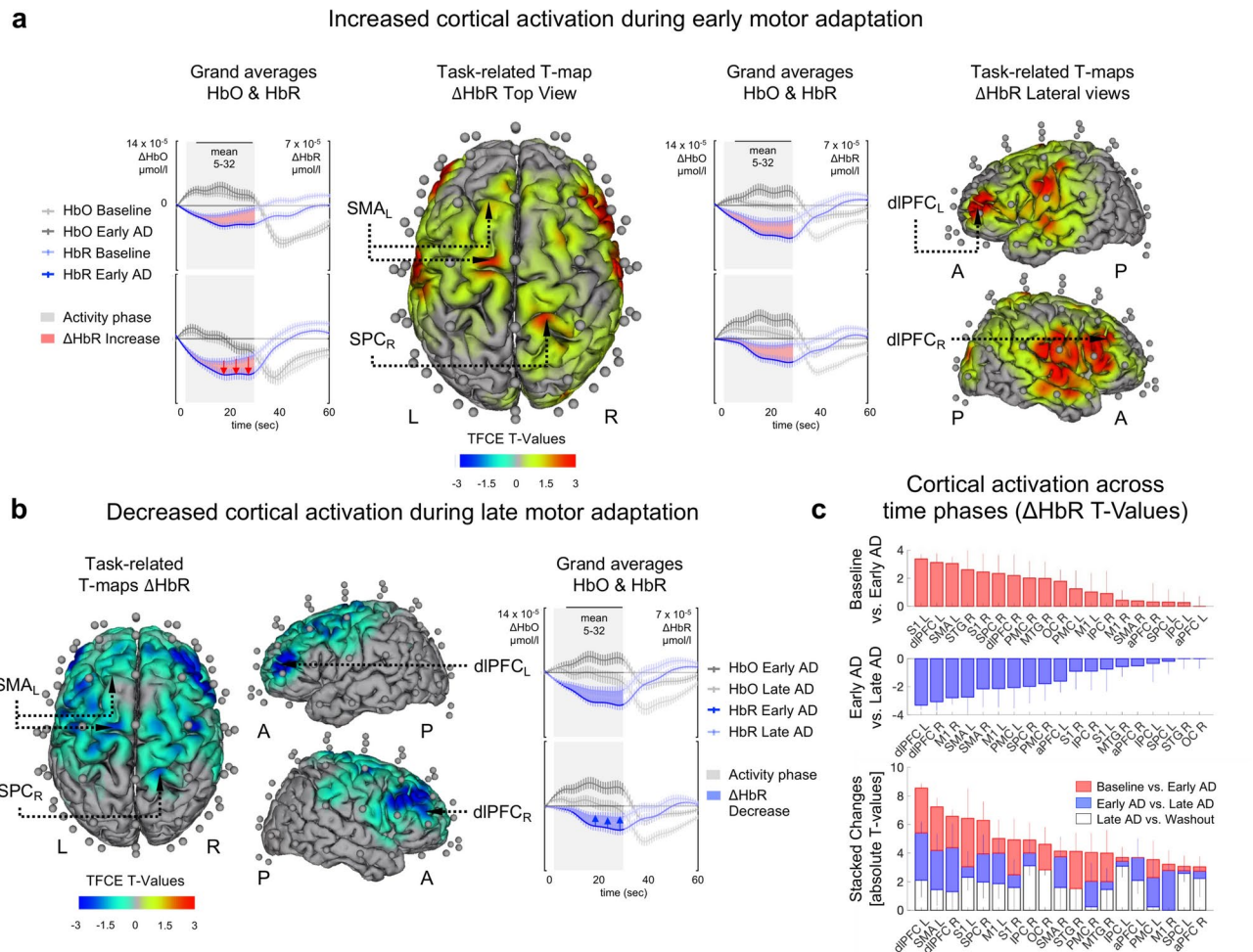
Fig. 4. Adaptation-dependent hemodynamic response alterations during table tennis. Line Plots: Grand-averages (HbO & HbR) for ROIs with highest TFCE t-values across time phases. Gray shaded area represents activity phase (0–32 s). T-maps: Temporal aggregated task-related TFCE t-values (HbR). Optodes (transmitters & detectors) are shown for topographic images (created with brain function mapping tool[34]); colors represent mean TFCE t-values (sample range 5–32 s). Images are thresholded at p < 0.05. (**a**) Baseline vs. early adaptation. Red shaded areas between HbR concentration changes as well as topographic difference maps show increased HbR concentration changes during early adaptation compared to baseline indicating higher cortical activation during early adaptation ($S1_L$, $t(37)_{max} = 6.09$, $p_{max} < .001$). (**b**) Early adaptation vs. late adaptation. Blue shaded area between HbR concentration changes as well as topographic difference maps indicate decreased activation during late adaptation compared to early adaptation ($dlPFC_R$, $t(37)_{max} = 5.20$, $p_{max} < .001$). (**c**) Cortical activation across time phases (sorted by TFCE t-values). Upper panel: Baseline vs. early adaptation, Centre panel: Early adaptation vs. late adaptation, Lower panel: Summarizing TFCE post hoc comparisons of HbR concentration changes (stacked changes: baseline vs. early AD, early AD vs. late AD, late AD vs. washout), largest overall adaptation-related changes were observed for $dlPFC_L$, SMA_L, $dlPFC_R$, $S1_L$, SPC_R, $M1_L$, $S1_R$, IPC_R, & OC_R. *AD* adaptation, *TFCE* threshold-free cluster enhancement, *A* anterior, *P* posterior, *L* left hemisphere, *R* right hemisphere.

Regarding HbO concentration changes also indicated higher cortical activation during early adaptation compared to baseline in a widespread cluster (STG_L, $t(37)_{max} = 8.29$, $p_{max} < 0.001$) including STG_L, $S1_R$, $S1_L$, STG_R, MTG_L, MTG_R, $Broca_R$, ITG_L, OC_L, $dlPFC_R$, $aPFC_R$, $Broca_L$, PMC_L, $dlPFC_L$, IPC_L, $M1_R$, OC_R, ITG_R, SPC_R, IPC_R, $M1_L$, PMC_R, $aPFC_L$, SPC_L & SMA_R (85 channels, sorted by TFCE t-values in descending order). HbO also indicated lower cortical activation during late adaptation compared to early adaptation ($aPFC_L$, $t(37)_{max} = 6.07$, $p_{max} < 0.001$) including $dlPFC_R$, $aPFC_R$, PMC_R, ITG_L, PMC_L, $Broca_L$, $dlPFC_L$, SPC_R, STG_L, IPC_L, IPC_R, OC_L, SPC_L, $Broca_R$, $aPFC_L$, OC_R, $M1_R$, STG_R, SMA_R, $S1_L$, $M1_L$, ITG_R, MTG_R, MTG_L & $S1_R$ (102 channels, sorted by TFCE t-values in descending order). Summarizing TFCE post hoc comparisons of HbO concentration changes (TFCE t-values summed across time phases: baseline vs. early adaptation, early vs. late adaptation, late adaptation vs. washout), largest overall adaptation-related changes were observed for STG_R, MTG_R, $Broca_L$, STG_L, $Broca_R$, $S1_R$, $dlPFC_R$, $S1_L$, $aPFC_R$ & ITG_L.

Psychological and physiological confounders

Statistical analysis of questionnaires revealed a significant increase for participants' discomfort (pre: 1.0 ± 0.0 [median ± MAD], post: 2.5 ± 0.5, Wilcoxon signed-rank tests: $z = -5.28$, $p < 0.001$). However, regarding attention (pre: 8.0 ± 1.0, post: 7.0 ± 1.0, $z = 0.73$, $p = 0.458$) and fatigue level (pre: 7.0 ± 1.0, post: 7.0 ± 1.0, $z = -1.622$, $p = 0.098$), there was no pre-post difference. There were no statistically significant differences between type of perturbation (serial vs. random) concerning pretest (Mann–Whitney U tests: attention: $p = 0.062$, $U = 283.0$, fatigue: $p = 0.129$, $U = 300.5$, discomfort: $p = 0.804$, $U = 404.5$), posttest (attention: $p = 0.050$, $U = 276.0$, fatigue: $p = 0.052$, $U = 276.0$, discomfort: $p = 0.926$, $U = 385.5$), or pre–posttest differences (attention: $p = 1.00$, $U = 391.5$, fatigue: $p = 0.838$, $U = 379.0$, discomfort: $p = 0.515$, $U = 430.5$).

Concerning cardiac stress operationalized via heart rate recordings during the execution of the table tennis strokes, there were no difference between groups (mean ± SD: Serial group: 92.50 ± 12.86 bpm, Random group: 88.32 ± 12.38 bpm; $F(1, 54) = 1.60$, $p = 0.211$, $\eta_p^2 = 0.03$) and no interaction between time and group ($F(1.98, 106.82) = 1.40$, $p = 0.250$, $\eta_p^2 = 0.001$). In contrast, the comparison of cardiac stress during baseline, early and late adaptation as well as deadaptation indicated lower heart rates during baseline (baseline: 87.98 ± 12.89 bpm, early adaptation: 91.13 ± 13.04 bpm, late adaptation: 91.25 ± 12.24 bpm; $F(1.98, 106.82) = 12.72$, $p < 0.001$, $\eta_p^2 = 0.01$, Post Hoc baseline—early adaptation: $t(55) = -4.68$, $p_{holm} < 0.001$, d = -0.25, early adaptation—late adaptation: $t(55) = -0.15$, p_{holm} 1.000, d = -0.01). Even when heart rate is added as a covariate to the model, HbR and HbO response alterations still show a significant increase from baseline to early adaptation (fNIRS subsample, $n = 38$, all channels; HbR: $F(1, 36) = 5.90$, $p = 0.020$, $\eta_p^2 = 0.14$; HbO: $F(1, 36) = 29.36$, $p < 0.001$, $\eta_p^2 = 0.45$), indicating an effect independent from heart rate alterations. In addition, covariance analyses were conducted for those channels forming a cluster with significant HbR resp. HbO increases (see previous section). Again, the adaptation dependent increase remains after controlling for the effect of heart rate alterations (HbR: $F(1, 36) = 9.32$, $p = 0.004$, $\eta_p^2 = 0.21$; HbO: $F(1, 36) = 41.29$, $p < 0.001$, $\eta_p^2 = 0.53$).

Discussion

The aim of the present study was to unravel cortical activation during motor adaptation in a sport-specific table tennis setting. While earlier (neuro-)behavioral studies have explored motor adaptation and neural correlates in restricted laboratory settings[21,53], we are aiming to adress everyday scenarios or sport-specific tasks that involve more complex processes, including various cognitive components and strategic corrections.

In line with our first hypothesis, we observed that (a) cortical structures, in particular, bilateral dlPFC, S1 & PMC, SMA$_L$ & M1$_L$ as well as SPC$_R$ and IPC$_R$ dynamically alter their activation as motor adaptation progresses. Specifically, in alignment with theoretical models and laboratory evidence (b) hemodynamic response alterations generally increased during early adaptation and decreases as visuomotor adaptation progresses. Contrary to our assumption, we observed further decreases during washout phase. In accordance with findings of our previous study[8], we observed typical adaptation-dependent performance changes and the temporal order of perturbations did not influence the process of motor adaptation (hypothesis c). Serial and randomized practice lead to non-differential performance changes and cortical activation.

ROIs showing adaptation-related response alterations

We observed dynamical changes in cortical activation in bilateral dlPFC, bilateral S1 and bilateral PMC. Furthermore, we identified dynamical changes in SMA$_L$ and M1$_L$ as well as SPC$_R$ and IPC$_R$ throughout the adaptation process. The pronounced alterations in bilateral dlPFC and bilateral S1 corroborate the findings of Shadmehr and Holcomb[5,54]. These authors discovered that at the initial stage of the learning process, the capacity of individuals to adapt to a disturbing force field is linked to an elevated activation in the left putamen and bilateral dlPFC. Furthermore, according to the aforementioned study, in the subsequent stages of the adaptation process, the comparison of initial and final learning conditions revealed an activation decline in the left and right sensorimotor cortex and right putamen. We observed an activation increase in bilateral S1 and M1$_L$ during early adaptation when compared to baseline and an activation decrease during late adaptation when compared to early adaptation. Moreover, such adaptation-related changes were observed in the SMA$_L$. Shadmehr und Holcomb[5,54] posit, given the significant projections from the sensorimotor cortex to the putamen, that changes observed in these regions are likely related to large-scale reductions in motor output rather than to the acquisition of an internal model. The majority of recent empirical studies have attributed the stepwise encoding of an internal model for novel visuomotor transformations to prefrontal and PPC areas[55]. In this context, our results reinforce the significance of the bilateral dlPFC, where in addition to the initial increase in activation a subsequent decrease in activation was observed.

Furthermore, our investigation of a motor adaptation task in a sport-specific context provides evidence that dynamic alterations occur in PPC throughout the adaptation phase. These findings are specific to the SPC$_R$ and the IPC$_R$. Generally speaking, the PPC, SPC in particular, facilitates sensorimotor integration by receiving multimodal input from the primary sensory cortex and output from the cerebellum. The IPC is responsible for new sensorimotor transformations and reference maps for spatial orientation and navigation[7]. We observed alterations in the SPC$_R$ during early and late adaptation. These findings confirm results from a recent fNIRS study[7], which suggests that the right posterior parietal cortex (rPPC) may be responsible for the establishment of a visuomotor transformation in the early stages of adaptation. Moreover, lesion studies suggest that rPPC may be specialized for spatial somatosensory function. Moreover, a number of studies have demonstrated the particular importance of the rPPC in the context of visual-spatial attention[56].

Finally, dPMC is also known to integrate proprioceptive and visual information[17]. When learning new visuomotor associations, both dPMC's neural activity and cerebellar activation increased[17] (Doyon et al., 2002). According to Tzvi et al.[17], the cerebellar dPMC loop has a unique role in controlling the process of visuomotor adaptation. Thus, the dPMC seems to perform visuomotor integration, while the cerebellum most likely

represents the internal model of motion. Furthermore, it has been proposed by Hardwick et al. (2015) that dPMC serves as a bridge between visuomotor control and higher cognitive functions during motor learning.

Direction of the adaptation-related response alterations

Research using fMRI has shown that cerebral activation increases in response to a sudden exposure to a visuomotor rotation, decreases as motor adaptation progresses, and increases again when the rotation is suddenly removed[17,57]. Furthermore, findings using fNIRS indicated that cortical activation initially increased and subsequently decreased after visuomotor adaptation occurs[7,55]. Taken together, empirical evidence suggest, that motor adaptations are linked to enhanced cognitive brain processing. Contrary to our original assumption, we observed decreasing activation during washout phase. This reduced cortical activation may be attributed to the fact that, in contrast to the adaptation phase, after-effects only occur for a brief period and can only be observed to a limited extent with our fNIRS methodology. As evidenced by behavioral data, the occurrence of significant errors is predominantly confined to the initial stage of the washout phase, specifically the initial block (W1). From the second washout-block onward, only minor kinematic errors were observed. However, the observed changes in cortical activation were averaged over five blocks (W1-W5). Therefore, fNIRS block averages do not only reflect a potentially activation increase in W1, but rather an overall enhancement in cortical brain processing across blocks W1-W5.

Serial vs. randomized practice

In contrast to our previous study, we standardized the number of task switches in the current study. We induced eight task switches in both the random order and the serial order group. Even with this standardized number of switches, we confirm that serial and randomized practice causes comparable contextual interference[58–60]. Also, our observations of cortical brain processing support this finding since serial and randomized practice induce similar changes in brain processing. This finding contradicts our original hypothesis, in which we suspected serial practice to induce higher cortical activation in regions responsible for working memory and sequence integration such as the PFC and SMA. However, according to the action plan reconstruction hypothesis, trial-by-trial skill variations necessitate retrieving information from long-term memory, independent from the factor predictability[61]. Even if participants noticed a predictability in the serial practice schedule, they never the less had to continuously build new motor action plans in each consecutive trial. This is also supported by our behavioral data, which clearly shows comparable contextual interference in both conditions. Furthermore, it might well be that participants didn´t even realized that the serial practice condition included repetitive trials.

The current study is also subject to some constraints. Even though subcortical structures are crucial for motor adaptation, with fNIRS neuroimaging only hemodynamic changes in cortical layers can be detected, making it impossible to determine if motor adaptation also affects subcortical activation (e.g., basal ganglia)[21,25,57,62]. Furthermore, kinematic observations may provide important additional information on the learning process. Particularly changes in hand movement (inclination of the table tennis racket) can be added to the current paradigm relatively easy and may provide important details of the actual movement adaptation. Additionally, the shift from baseline to early motor adaptation phase is not only characterized by a change from topspin (baseline) to backspin (early adaptation) but also by a shift from blocked practice (single ball velocity) to serial or random practice (changing ball velocities). Therefore, contrasting baseline and early adaptation phase in terms of cortical activation does not only portray neural adaptation to the perturbation spin and slightly changing ball trajectories due to the magnus effect but also neural adaptation to the perturbation ball length, induced by changing ball velocities. This was done to increase task complexity to ensure a slow and lasting motor adaptation process that is detectable over a long period of time using our blocked fNIRS protocol. Nevertheless, we observed that these induced complex perturbations led to typical behavioral adaptations, thus would conclude that they also induce typical neural adaptation. Also, the contrast early vs. late adaptation is not affected by this methodological limitation, since in both phases similar complex perturbations were presented. We used a ball robot to standardize the movement task as much as possible. However, this standardization also at least to some extend limits the movement task as compared to match conditions during a real table tennis game. Here, the game situation is constantly changing and the player has to anticipate which shot will be taken next. Technical and tactical information provides clues which action will be performed next (e.g., the opponent's posture).

Finally, participants reported an increase in discomfort during the time course of the experiment. This in turn might have affected our fNIRS data as well. However, due to the dynamical nature of cortical activation during motor adaptation it seems unlikely that pain-associated brain activation might have contrasted our main findings. Nevertheless, future studies have to be designed to limit the influence of pain-related discomfort and associated brain activations.

Conclusion

Our whole-head fNIRS study was not only able to demonstrate the involvement of selected regions of interest, e.g., PPC[7], during motor adaptations. Moreover, it furnished a more comprehensive representation of the continuously evolving cortical activation. In sum, our analysis of cortical brain processing during a complex sport-specific task (in a standing position) corroborates the findings of neurobehavioral studies that observed simple movement tasks under strictly controlled laboratory conditions (in a lying or sitting position).

Our findings revealed that cortical structures, particularly the bilateral dlPFC and S1, the SMA_L and $M1_L$, as well as the SPC_R and IPC_R, exhibited a dynamic alteration in their activation as motor adaptation progresses. In alignment with theoretical models and laboratory evidence, hemodynamic response alterations generally increased during early adaptation and decreased as visuomotor adaptation progressed. Furthermore, the temporal order of perturbations did not influence the process of motor adaptation. Serial and randomized

practice led to the same performance changes. Additionally, no differential changes in cortical brain processing were observed with serial and randomized practice.

Data availability

All data that support the findings of this study are available from the corresponding author, D.C. if a formal data sharing agreement exists. Besides, all software used in the present study is open-source and as such publicly available.

References

1. Brashers-Krug, T., Shadmehr, R. & Bizzi, E. Consolidation in human motor memory. *Nature* **382**, 252–255. https://doi.org/10.1038/382252a0 (1996).
2. Heald, J. B., Lengyel, M. & Wolpert, D. M. Contextual inference underlies the learning of sensorimotor repertoires. *Nature* **600**, 489–493. https://doi.org/10.1038/s41586-021-04129-3 (2021).
3. Imamizu, H. et al. Human cerebellar activity reflecting an acquired internal model of a new tool. *Nature* **403**, 192–195. https://doi.org/10.1038/35003194 (2000).
4. Kording, K. P. & Wolpert, D. M. Bayesian integration in sensorimotor learning. *Nature* **427**, 244–247. https://doi.org/10.1038/nature02169 (2004).
5. Shadmehr, R. & Holcomb, H. H. Neural correlates of motor memory consolidation. *Science* **277**, 821–825 (1997).
6. McDougle, S. D. & Taylor, J. A. Dissociable cognitive strategies for sensorimotor learning. *Nat. Commun.* **10**, 40. https://doi.org/10.1038/s41467-018-07941-0 (2019).
7. Yeo, S. S., Jang, T. S. & Yun, S. H. Sensorimotor adaptation in spatial orientation task: a fNIRS study. *Sci. Rep.* **13**, 15160. https://doi.org/10.1038/s41598-023-42416-3 (2023).
8. Carius, D. et al. Quantifying motor adaptation in a sport-specific table tennis setting. *Sci. Rep.* **14**, 601. https://doi.org/10.1038/s41598-023-50927-2 (2024).
9. Taylor, J. A., Krakauer, J. W. & Ivry, R. B. Explicit and implicit contributions to learning in a sensorimotor adaptation task. *J. Neurosci.* **34**, 3023–3032. https://doi.org/10.1523/JNEUROSCI.3619-13.2014 (2014).
10. Heald, J. B., Lengyel, M. & Wolpert, D. M. Contextual inference in learning and memory. *Trends Cogn. Sci.* **27**, 43–64. https://doi.org/10.1016/j.tics.2022.10.004 (2023).
11. Shadmehr, R. & Mussa-Ivaldi, F. A. Adaptive representation of dynamics during learning of a motor task. *J. Neurosci.* **14**, 3208–3224. https://doi.org/10.1523/JNEUROSCI.14-05-03208.1994 (1994).
12. Herzfeld, D. J., Vaswani, P. A., Marko, M. K. & Shadmehr, R. A memory of errors in sensorimotor learning. *Science* **345**, 1349–1353. https://doi.org/10.1126/science.1253138 (2014).
13. Shadmehr, R. & Brashers-Krug, T. Functional stages in the formation of human long-term motor memory. *J. Neurosci.* **17**, 409–419. https://doi.org/10.1523/JNEUROSCI.17-01-00409.1997 (1997).
14. Sheahan, H. R., Franklin, D. W. & Wolpert, D. M. Motor planning, not execution, separates motor memories. *Neuron* **92**, 773–779. https://doi.org/10.1016/j.neuron.2016.10.017 (2016).
15. Galea, J. M., Vazquez, A., Pasricha, N., de Xivry, J. J. & Celnik, P. Dissociating the roles of the cerebellum and motor cortex during adaptive learning: the motor cortex retains what the cerebellum learns. *Cereb. Cortex* **21**, 1761–1770. https://doi.org/10.1093/cercor/bhq246 (2011).
16. Heuer, H. & Hegele, M. Adaptation to visuomotor rotations in younger and older adults. *Psychol. Aging* **23**, 190–202. https://doi.org/10.1037/0882-7974.23.1.190 (2008).
17. Tzvi, E., Koeth, F., Karabanov, A. N., Siebner, H. R. & Kramer, U. M. Cerebellar—Premotor cortex interactions underlying visuomotor adaptation. *Neuroimage* **220**, 117142. https://doi.org/10.1016/j.neuroimage.2020.117142 (2020).
18. Wolpe, N. et al. Age-related reduction in motor adaptation: brain structural correlates and the role of explicit memory. *Neurobiol. Aging* **90**, 13–23. https://doi.org/10.1016/j.neurobiolaging.2020.02.016 (2020).
19. Lage, G. M., Faria, L. O., Ambrósio, N. F. A., Borges, A. M. P. & Apolinário-Souza, T. What Is the level of contextual interference in serial practice? A meta-analytic review. *J. Motor Learn. Dev.* **10**, 224–242. https://doi.org/10.1123/jmld.2021-0020 (2022).
20. Lelis-Torres, N., Ugrinowitsch, H., Apolinario-Souza, T., Benda, R. N. & Lage, G. M. Task engagement and mental workload involved in variation and repetition of a motor skill. *Sci. Rep.* **7**, 14764. https://doi.org/10.1038/s41598-017-15343-3 (2017).
21. Tzvi, E., Loens, S. & Donchin, O. Mini-review: The role of the cerebellum in visuomotor adaptation. *Cerebellum* **21**, 306–313. https://doi.org/10.1007/s12311-021-01281-4 (2022).
22. Doyon, J., Penhune, V. & Ungerleider, L. G. Distinct contribution of the cortico-striatal and cortico-cerebellar systems to motor skill learning. *Neuropsychologia* **41**, 252–262. https://doi.org/10.1016/s0028-3932(02)00158-6 (2003).
23. Krebs, H. I. et al. Robot-aided functional imaging: application to a motor learning study. *Hum. Brain Mapp.* **6**, 59–72. https://doi.org/10.1002/(SICI)1097-0193(1998)6:1 (1998).
24. Gottlieb, J. From thought to action: the parietal cortex as a bridge between perception, action, and cognition. *Neuron* **53**, 9–16. https://doi.org/10.1016/j.neuron.2006.12.009 (2007).
25. Bedard, P. & Sanes, J. N. Brain representations for acquiring and recalling visual-motor adaptations. *Neuroimage* **101**, 225–235. https://doi.org/10.1016/j.neuroimage.2014.07.009 (2014).
26. Debas, K. et al. Brain plasticity related to the consolidation of motor sequence learning and motor adaptation. *Proc. Natl. Acad. Sci. USA* **107**, 17839–17844. https://doi.org/10.1073/pnas.1013176107 (2010).
27. Herold, F. et al. Functional near-infrared spectroscopy in movement science: a systematic review on cortical activity in postural and walking tasks. *Neurophotonics* **4**, 041403. https://doi.org/10.1117/1.NPh.4.4.041403 (2017).
28. Hamacher, D., Herold, F., Wiegel, P., Hamacher, D. & Schega, L. Brain activity during walking: A systematic review. *Neurosci. Biobehav. Rev.* **57**, 310–327. https://doi.org/10.1016/j.neubiorev.2015.08.002 (2015).
29. Dayan, E. & Cohen, L. G. Neuroplasticity subserving motor skill learning. *Neuron* **72**, 443–454. https://doi.org/10.1016/j.neuron.2011.10.008 (2011).
30. Oldfield, R. C. The assessment and analysis of handedness: The Edinburgh inventory. *Neuropsychologia* **9**, 97–113. https://doi.org/10.1016/0028-3932(71)90067-4 (1971).
31. Dragovic, M. Categorization and validation of handedness using latent class analysis. *Acta Neuropsychiatr.* **16**, 212–218. https://doi.org/10.1111/j.0924-2708.2004.00087.x (2004).
32. Peirce, J. W. PsychoPy–psychophysics software in python. *J. Neurosci. Methods* **162**, 8–13. https://doi.org/10.1016/j.jneumeth.2006.11.017 (2007).
33. Carius, D. et al. Increased cortical activity in novices compared to experts during table tennis: A whole-brain fnirs study using threshold-free cluster enhancement analysis. *Brain Topogr.* https://doi.org/10.1007/s10548-023-00963-y (2023).

34. Wang, Y., Yan, J., Wen, J., Yu, T. & Li, X. An Intracranial electroencephalography (iEEG) brain function mapping tool with an application to epilepsy surgery evaluation. *Front. Neuroinform.* **10**, 15. https://doi.org/10.3389/fninf.2016.00015 (2016).

35. ZimeoMorais, G. A., Balardin, J. B. & Sato, J. R. fNIRS optodes' location decider (fOLD): a toolbox for probe arrangement guided by brain regions-of-interest. *Sci. Rep.* **8**, 3341. https://doi.org/10.1038/s41598-018-21716-z (2018).

36. Huppert, T. J., Diamond, S. G., Franceschini, M. A. & Boas, D. A. HomER: a review of time-series analysis methods for near-infrared spectroscopy of the brain. *Appl. Opt.* **48**, 280–298. https://doi.org/10.1364/AO.48.00D280 (2009).

37. Hernandez, S. M. & Pollonini, L. NIRSplot: A tool for quality assessment of fNIRS scans. *Biomed. Opt. 2020* https://doi.org/10.1364/BRAIN.2020.BM2C.5 (2020).

38. Brigadoi, S. et al. Motion artifacts in functional near-infrared spectroscopy: a comparison of motion correction techniques applied to real cognitive data. *NeuroImage* **85** (1), 181–191. https://doi.org/10.1016/j.neuroimage.2013.04.082 (2014).

39. Di Lorenzo, R. et al. Recommendations for motion correction of infant fNIRS data applicable to multiple data sets and acquisition systems. *NeuroImage* **200**, 511–527. https://doi.org/10.1016/j.neuroimage.2019.06.056 (2019).

40. Molavi, B. & Dumont, G. A. Wavelet-based motion artifact removal for functional near-infrared spectroscopy. *Physiol. Meas.* **33**, 259–270. https://doi.org/10.1088/0967-3334/33/2/259 (2012).

41. Carius, D., Hörnig, L., Ragert, P. & Kaminski, E. Characterizing cortical hemodynamic changes during climbing and its relation to climbing expertise. *Neurosci. Lett.* **715**, 134604. https://doi.org/10.1016/j.neulet.2019.134604 (2020).

42. Yücel, M. A. et al. Best practices for fNIRS publications. *Neurophotonics* **8**, 012101. https://doi.org/10.1117/1.NPh.8.1.012101 (2021).

43. Tachtsidis, I. & Scholkmann, F. False positives and false negatives in functional near-infrared spectroscopy: issues, challenges, and the way forward. *Neurophotonics* **3**, 030401. https://doi.org/10.1117/1.NPh.3.3.030401 (2016).

44. Dravida, S., Noah, J. A., Zhang, X. & Hirsch, J. Comparison of oxyhemoglobin and deoxyhemoglobin signal reliability with and without global mean removal for digit manipulation motor tasks. *Neurophotonics* **5**, 011006. https://doi.org/10.1117/1.NPh.5.1.011006 (2018).

45. Kirilina, E. et al. The physiological origin of task-evoked systemic artefacts in functional near infrared spectroscopy. *NeuroImage* **61**, 70–81. https://doi.org/10.1016/j.neuroimage.2012.02.074 (2012).

46. Huppert, T. J., Hoge, R. D., Dale, A. M., Franceschini, M. A. & Boas, D. A. Quantitative spatial comparison of diffuse optical imaging with blood oxygen level-dependent and arterial spin labeling-based functional magnetic resonance imaging. *J. Biomed. Opt.* **11**, 064018. https://doi.org/10.1117/1.2400910 (2006).

47. Huppert, T. J., Hoge, R. D., Diamond, S. G., Franceschini, M. A. & Boas, D. A. A temporal comparison of BOLD, ASL, and NIRS hemodynamic responses to motor stimuli in adult humans. *NeuroImage* **29**, 368–382. https://doi.org/10.1016/j.neuroimage.2005.08.065 (2006).

48. Plichta, M. M. et al. Event-related functional near-infrared spectroscopy (fNIRS) based on craniocerebral correlations: reproducibility of activation?. *Hum. Brain Mapp.* **28**, 733–741. https://doi.org/10.1002/hbm.20303 (2007).

49. Lühmann, A., Ortega-Martinez, A., Boas, D. A. & Yücel, M. A. Using the general linear model to improve performance in fnirs single trial analysis and classification: A perspective. *Front. Hum. Neurosci.* **14**, 30. https://doi.org/10.3389/fnhum.2020.00030 (2020).

50. Yücel, M. A. et al. Specificity of hemodynamic brain responses to painful stimuli: a functional near-infrared spectroscopy study. *Sci. Rep.* **5**, 9469. https://doi.org/10.1038/srep09469 (2015).

51. Mensen, A. & Khatami, R. Advanced EEG analysis using threshold-free cluster-enhancement and non-parametric statistics. *Neuroimage* **67**, 111–118. https://doi.org/10.1016/j.neuroimage.2012.10.027 (2013).

52. Smith, S. M. & Nichols, T. E. Threshold-free cluster enhancement: addressing problems of smoothing, threshold dependence and localisation in cluster inference. *Neuroimage* **44**, 83–98. https://doi.org/10.1016/j.neuroimage.2008.03.061 (2009).

53. Reuter, E. M., Booms, A. & Leow, L. A. Using EEG to study sensorimotor adaptation. *Neurosci. Biobehav. Rev.* **134**, 104520. https://doi.org/10.1016/j.neubiorev.2021.104520 (2022).

54. Shadmehr, R. & Holcomb, H. H. Inhibitory control of competing motor memories. *Exp. Brain Res.* **126**, 235–251. https://doi.org/10.1007/s002210050733 (1999).

55. Gentili, R. J., Shewokis, P. A., Ayaz, H. & Contreras-Vidal, J. L. Functional near-infrared spectroscopy-based correlates of prefrontal cortical dynamics during a cognitive-motor executive adaptation task. *Front. Hum. Neurosci.* **7**, 277. https://doi.org/10.3389/fnhum.2013.00277 (2013).

56. Sengupta, A., Banerjee, S., Ganesh, S., Grover, S. & Sridharan, D. The right posterior parietal cortex mediates spatial reorienting of attentional choice bias. *Nat. Commun.* **15**, 6938. https://doi.org/10.1038/s41467-024-51283-z (2024).

57. Tzvi, E., Gajiyeva, L., Bindel, L., Hartwigsen, G. & Classen, J. Coherent theta oscillations in the cerebellum and supplementary motor area mediate visuomotor adaptation. *Neuroimage* **251**, 118985. https://doi.org/10.1016/j.neuroimage.2022.118985 (2022).

58. Giuffrida, C., Shea, J. & Fairbrother, J. T. Differential transfer benefits of increased practice for constant, blocked, and serial practice schedules. *J. Mot. Behav.* **34**, 353–365. https://doi.org/10.1080/00222890209601953 (2002).

59. Keller, G. J., Li, Y., Weiss, L. W. & Relyea, G. E. Contextual interference effect on acquisition and retention of pistol-shooting skills. *Percept. Mot. Skills* **103**, 241–252. https://doi.org/10.2466/pms.103.1.241-252 (2006).

60. Sekiya, H. Contextual interference in implicit and explicit motor learning. *Percept. Mot. Skills* **103**, 333–343. https://doi.org/10.2466/pms.103.2.333-343 (2006).

61. Lee, T. D. & Magill, R. A. Can forgetting facilitate skill acquisition?. *Adv. Psychol.* **27**, 3–22. https://doi.org/10.1016/S0166-4115(08)62528-5 (1985).

62. Taylor, J. A. & Ivry, R. B. Cerebellar and prefrontal cortex contributions to adaptation, strategies, and reinforcement learning. *Prog. Brain Res.* **210**, 217–253. https://doi.org/10.1016/B978-0-444-63356-9.00009-1 (2014).

Author contributions

DC: Methodology, Conceptualization, Formal analysis, Investigation, Software, Visualization, Writing—original draft, Writing—review & editing. EK: Methodology, Conceptualization, Writing—review & editing. MC: Methodology. PR: Conceptualization, Resources, Supervision, Writing—review & editing.

Funding

Declarations

Competing interests

The authors declare no competing interests.

Additional information

Correspondence and requests for materials should be addressed to D.C.

Reprints and permissions information is available at www.nature.com/reprints.

Publisher's note Springer Nature remains neutral with regard to jurisdictional claims in published maps and institutional affiliations.